Supra 36 water in the Pacific Ocean[*]

Takashi ICHIYE[**] and Ping CHANG[**]

Abstract: In the eastern South Pacific east of 180 longitude and north of 30°S, high saline water with salinity 36 psu was found near and above 200m during JAPACS 1991 Cruise in Jan-March. In the whole Pacific Ocean this is the only water with that salinity range. LEVITUS (1982) salinity charts and TSUCHIYA's (1968) thermosteric charts indicate that water with the surface salinity above 36 psu between 150°W and 100°W may subduct at 130°W between equator and 10°S. Further subduction and sinking of high salinity water is helped by downwelling Ekman pumping south of the equator west of 160°E. The equation balancing horizontal advection and the vertical diffusion with its simple solution is applied to vertical salinity profiles at 4°S and 5°S of 160°W and 180°, yielding vertical diffusion coefficients order of $10^{-4}m^2/s$.

1. Introduction

During analysis of hydrographic data collected in JAPACS Cruise 1991 in the tropical Pacific Ocean by JAMSTEC we noticed that water with salinity above 36 psu was found only in sections of 160°W and 180°, but not 160°E nor east of it. The water was limited south of 3°S and to the depth of near and above 200 m (ANDO, et al., 1992, hereafter referred as AIM). Watermass census according to temperature and salinity by WORTHINGTON (1982) indicates water of salimity above 36 psu, belongs to rare species, forming only 16×10^6 km³ of the total global ocean water of 1320.5×10^6 km³. We called this water Supra 36 Water or S36W, sometimes simply SW. In the Pacific Ocean, SW exists only in the South Pacific. It seems worthwhile to examine this water, because the water is a good tracer as is the Mediterranean Outflow in the Atlantic. It also yields an example of formation of a watermass in the mid ocean.

2. Formation of SW in the South Pacific Ocean

Classical studies of MONTGOMERY (1958) and COCHRANE (1958) on T-S relations respectively on the world ocean and the Pacific Ocean demonstrated that in general salinity is less for the same temperature and depth in the Pacific than in the Atlantic Ocean.

High salinity water is produced at the surface layer in the ocean, in general. This feature of salinity difference between the oceans can be seen in climatological salinity distributions at the surface and at 150 m layer from charts prepared by LEVITUS (1982) (computer reproductions for 40°S-40°N are shown in Fig. 1.) These indicate that in the Pacific and Indian Oceans the SW is found only in the South Pacific Ocean and in a limited area of northwest Bay of Bengal off the mouth of Persian Gulf, whereas in the Atlantic Ocean the SW is in both hemispheres and occupies much wider areas.

Table 1 indicates the area of the SW at the surface and 150 m determined from LEVITUS' (1982) charts shown in Fig. 1. It is noted that the SW area is larger at 150 m than at the surface in the South Pacific Ocean, whereas in the South Atlantic the SW area at 150 m shrinks to half of the surface SW area. Later we will show that in the South Pacific Ocean subduction of the surface high salinity water is extensive and also downwelling due to Ekman pumping that extends westwards from near the eatern

Table 1. Areas of SW 36 from LEVITUS (1982) (unit 10^6 km²).

	Surface	at 150 m
South Pacific	61.5	100
N. Atlantic	248	308
S. Atlantic	141	71

DEPTH : 0m

DEPTH : 150m
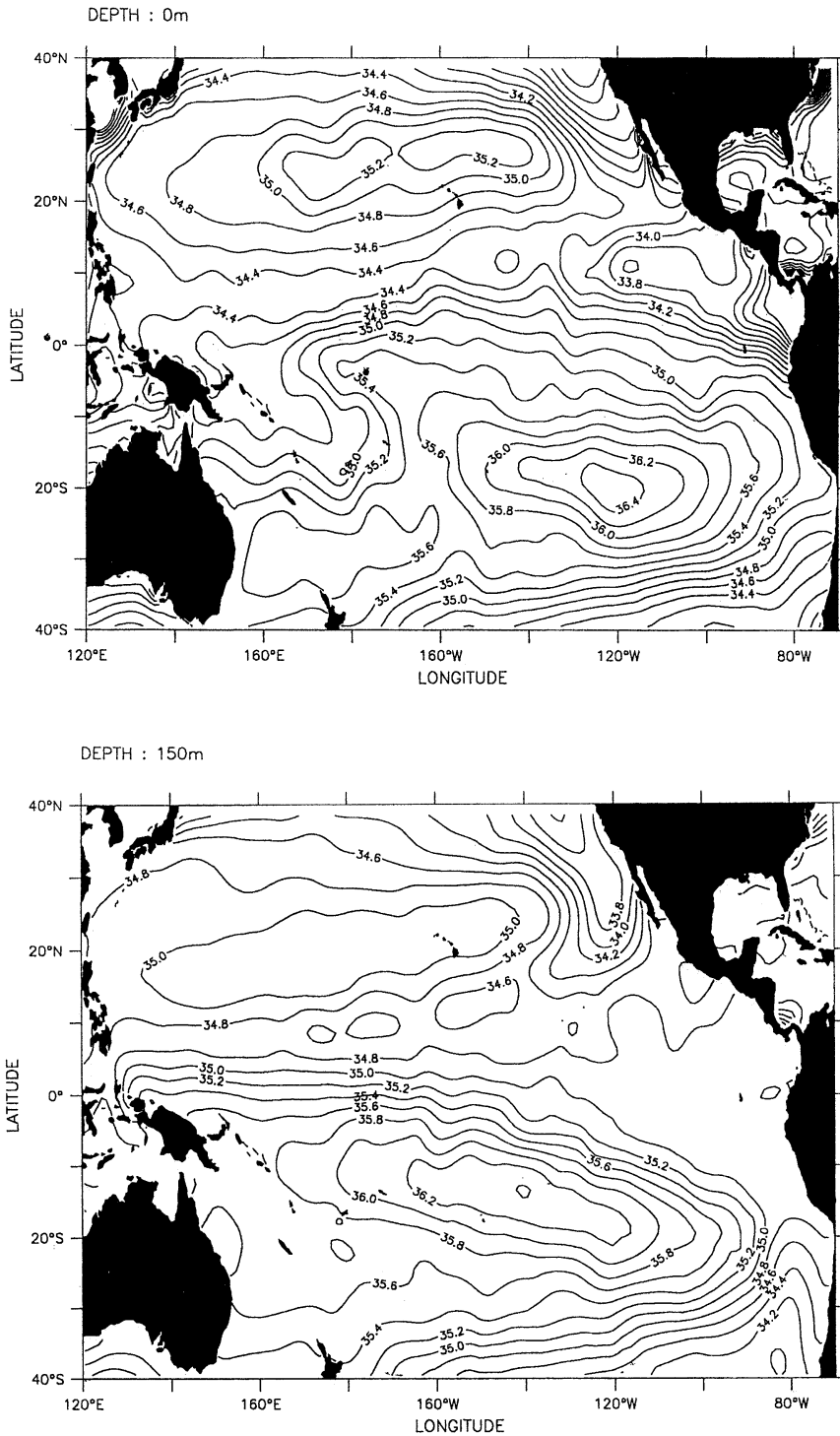
Fig. 1. Climatological salinity at 0 m and 150 m from LEVITUS (1982), modified
for 40°N to 40°S.
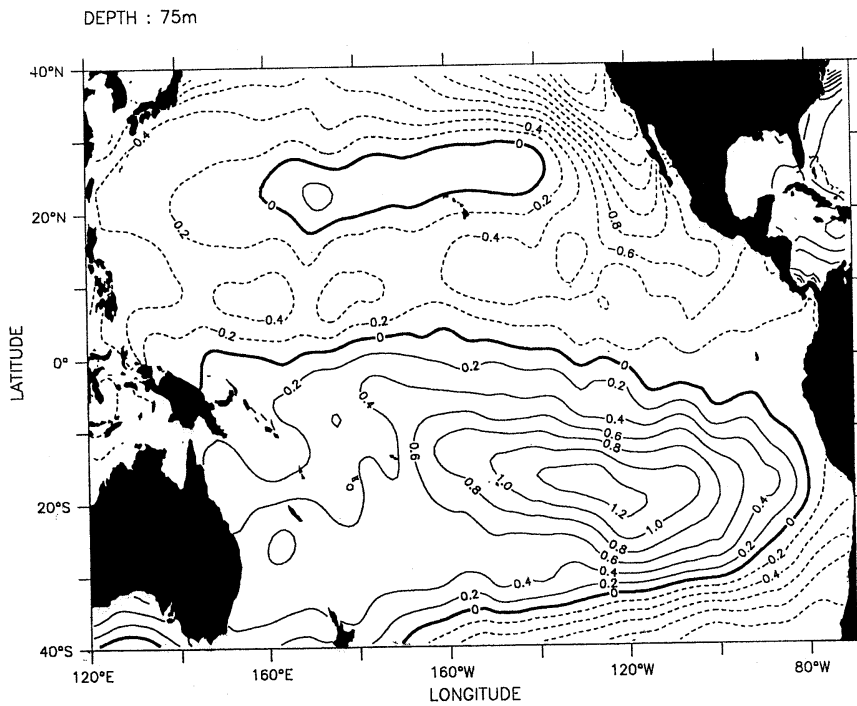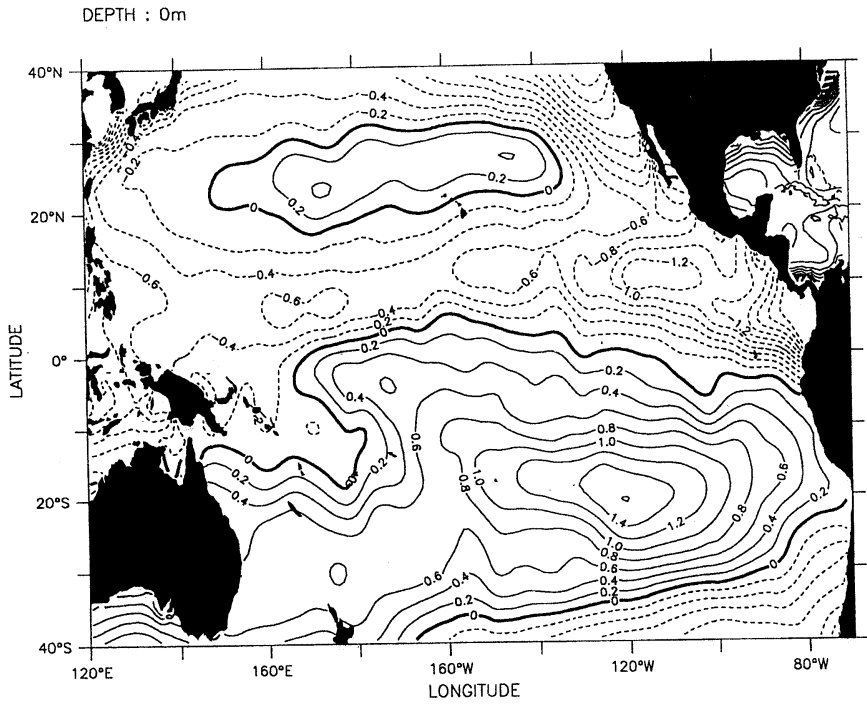
DEPTH : 0m

DEPTH : 75m

Fig. 2a and 2b. Salinity at 0 and 75 m subtracted the average over the Pacific between 40°N and 40°S based on LEVITUS' (1982) data.
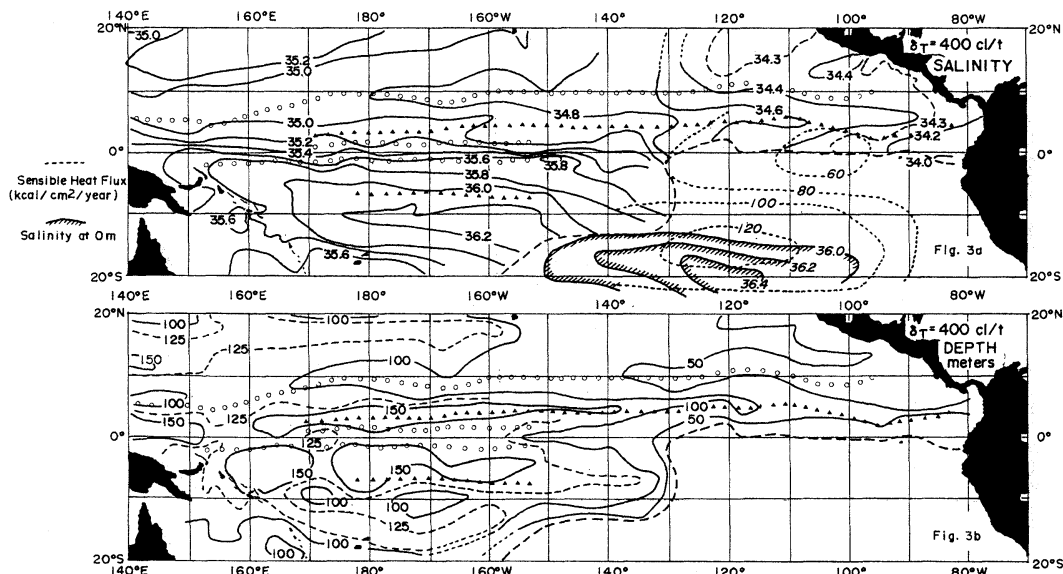
Fig. 3a and 3b. Salinity and depth at and of 400 cl/t thermosteric anomaly surface (TSUCHIYA,1968).
The axes of maxima and minima of acceleration potential are indicated by closed triangles and circles, respectively.
Full lines with hatch in Fig. 3a: Salinity at 0m from LEVITUS (1982). Shortdashed lines in Fig. 3 a: Sensible heat flux (k cal/cm²/year) from BUDYKO (1974). When divided by 600, the number equals evaportation minus precipitation in cm/cm²/year.

boundary to beyond 160° E, though the surface SW region is limited only east of 160° W. In the North Atlantic Ocean the Mediterranean outflow may contribute to extend the SW area at 150 m particularly through Supra 37 Water between 20° N and 30° N.

In order to show locations of high salinity water more clearly, salinity anomalies are determined from LEVITUS' (1982) data by subtracting the average of from 40° S and 40° N and over the Pacific Ocean at 0 m and 75 m and plotted in Fig. 2a and 2b, respectively. The latter depth is chosen to represent anomalies independent on atmospheric influences. These figures indicate positive anomalies dominate in the tropical South Pacific over the North Pacific with the difference of maximum values by 1.2 psu for both depths.

3. The surface SW and its subduction

In order to visualize formation of the surface SW area and its subduction, salinity and depth of 400 cl/t surface are shown from TSUCHIYA (1968) in Fig. 3a and 3b respectively. These

figures indicate that the 400 cl/t surface outcrops in the eastern part of the tropical South Pacific.

In Fig. 3a the surface salinity contours from LEVITUS (1982) are overlaid in the outcropped area together with the sensible heat flux contours from BUDYKO (1974) in kcal/cm²/year. The numbers in BUDYKO contours almost equal evaporation minus precipitation in cm/cm²/year when divided by 600. If surface salinity is produced simply by difference of evaporation (E) and precipitation (P) as in a standstill water body, then high salinity area and high E-P area should coincide. However, Fig. 3a indicates that the center of the high salinity area is about 530 km south of the high E-P area. This is speculated as a result of the Ekman pumping and surface current as discussed later.

In the context of ventilated thermocline models (LUYTEN et al, 1983), the SW is forced downwelling by the Ekman punping in the outcropped region. The pumping velocity at the bottom of the upper Ekman layer w_h is given by:
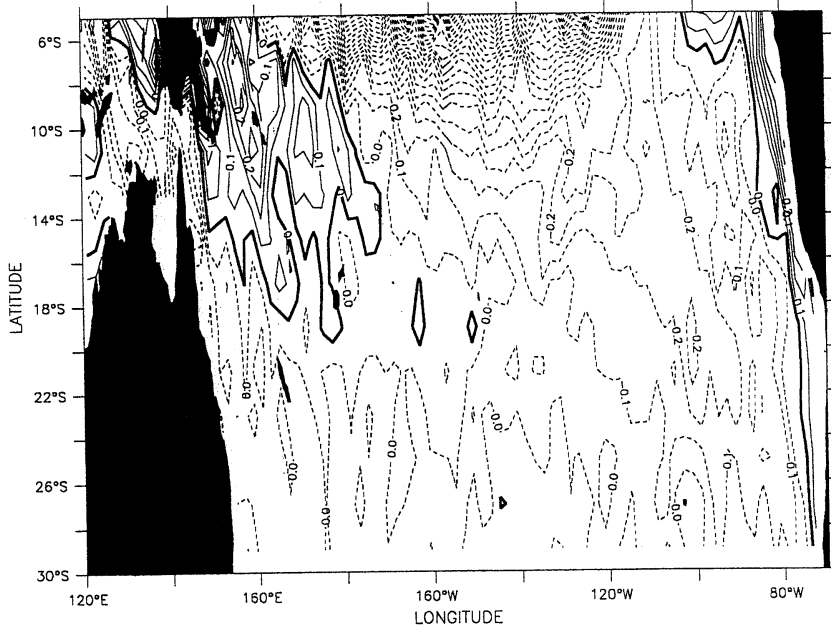
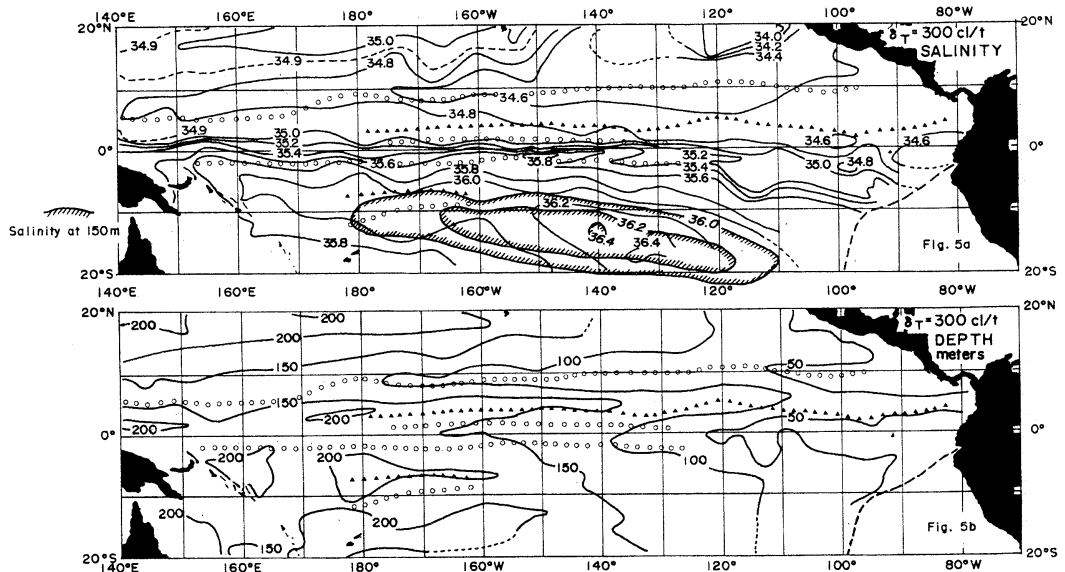Fig. 4. Ekman pumping velocity (10^{-5}cm/s) at 50 m. Full lines indicate upward, broken lines downward.

Fig. 5 a and 5b. Salinity (psu) and depth (m) at and of 300 cl/t thermosteric anomaly surface from TSUCHIYA (1968). Full lines with hatch in Fig. 5a show salinity at 150 m from LEVITUS (1982). The axes of maxima and minima of accelerated potential are indicated by closed triangles and circles, respectively.

$$w_h = \frac{\partial}{\partial y}\left(\frac{T_x}{f}\right) - \frac{\partial}{\partial x}\left(\frac{T_y}{f}\right) \qquad (1)$$

where T_x and T_y are eastward and northward components of the wind stress, respectively and f is the Coriolis parameter.

The distribution of w_h is shown in Fig. 4. The downwelling region of Ekman pumping extends
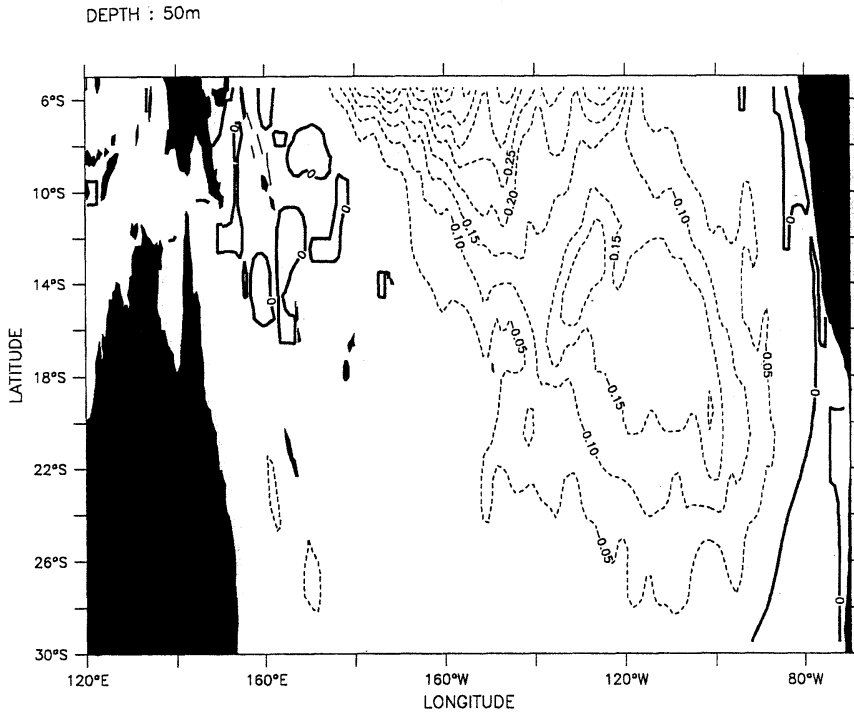
DEPTH : 50m

Fig. 6. Salt anomalies flux by Ekman pumping. (The mean salinity is taken from 5°S to
30°S and 120°E to 80°W, flux unit is psu x 10^{-5}cm/s.)

zonally from the east coast to 160°E with a decreasing width of velocity above 0.2×10^{-5} cm/s, though within 5° latitude of the equator equation (1) is not applicable because of f being close to zero. The westward extension of the downwelling zone explains the same pattern of the SW at the 400 cl/t surface together with the effect of the westward subduction flow. The depth and the salinity at 300 cl/t surface are shown in Fig. 5a and 5b, respecitvely. Also, in Fig. 5a salinity at 150m is shown from LEVITUS' (1982) chart.

When the surplus salinity is defined at $S-\bar{S}$, where $\bar{S}$ is the surface salinity averged over the South Pacific Ocean, the surplus salinity flux F_s due to the Ekman pumping is expressed by

$$F_s = \int w_h (S - \bar{S}) d\sigma \qquad (2)$$

the integral represents the whole surface of the South Pacific Ocean. Excess salinity flux chart is shown in Fig. 6, where reference depth of S and $\bar{S}$ is taken at 50 m instead of surface because the Ekman pumping w_h can be computed only at

this depth.

4. Mixing of the high salinity core

As Fig. 3a indicates, the salinity values in the core of the SW decreases downstream as the water is advected. This suggests that mixing processes are occurring, though subduction thermocline models are based on non-dissipative flow. By use of decrease of salinity in the core we can estimate the eddy diffusivity there.

Since the data available are rather crude, it is not possible to determine details of dissipative processes but it may be adequate to estimate an order of magnitude of such parameters. Conventional models of eddy diffusion depend on the gradients of materials, and only the vertical gradients of salinity can be estimated from the observed data, with some confidence. Therefore, only the vertical diffusion coefficient is treated.

A diffusion-advection equation

$$U \frac{\partial S}{\partial x} = \frac{\partial}{\partial z} \left(K \frac{\partial S}{\partial z} \right) \qquad (3)$$

Table 2. Depth differences Δh (in m) for $\Delta S = 0.2$ psu above and below salinity maximum determined from CTD profiles.

at 180°	above	$\Delta z = 7.8 \pm 2.5$
	below	$\Delta z = 8.8 \pm 2.8$
at 160°W	above	$\Delta z = 8.7 \pm 2.5$
	below	$\Delta z = 13.1 \pm 1.3$

is integrated vertically in the core of the SW, where U is the advection velocity, K is the eddy diffusivity and z is the vertical axis positively upward. Integration of (3) with z from $z = z_2$ (lower boundary) to $z = z_1$ (upper boundary) and averaging with depth leads to

$$\bar{U} \frac{\partial \bar{S}}{\partial x} = \frac{1}{h} \left[\left(K \frac{\partial S}{\partial z} \right)_1 - \left(K \frac{\partial S}{\partial z} \right) \right]_2 \quad (4)$$

where the bar indicates the vertically averaged values, h is the thickness of the core layer and suffices 1 and 2 represent the upper and lower boundary, respectively. The differential at the upper and lower boundary in equation (4) can be replaced with the difference $\Delta S / \Delta z$ to use observed salinity distributions. By taking $\Delta S = 0.2$ psu from AIM and using cross sections at 160°W and 180°, sectionally averaged values of vertical salinity gradients determined from the data are listed in Table 2. Although accuracy of $\partial \bar{S} / \partial x$ determined from the data is far from perfect because of a large distance between 160°W and 180°, the value of K from equation (4) is given by

$$K = U \times 1.37 \times 10^{-4} (\text{in m}^2/\text{s}) \quad (5)$$

with U between 0.1m/s and 0.5m/s, K is of the order of $10^{-5} \text{m}^2/\text{s}$ which is much larger than molecular diffusivity of $2 \times 10^{-8} \text{m}^2/\text{s}$ (SVERDRUP et al, 1945) but reasonable as the eddy diffusivity estimates by others.

Other estimates by curvefitting of an analytical form to vertical profiles of the observed salinity based on a model (CRANK, 1956) are presented in Appendix. Both estimates indicate that the eddy diffusivity is in practical terms small and the subduction may be treated as nondissipative processes except in frontal areas.

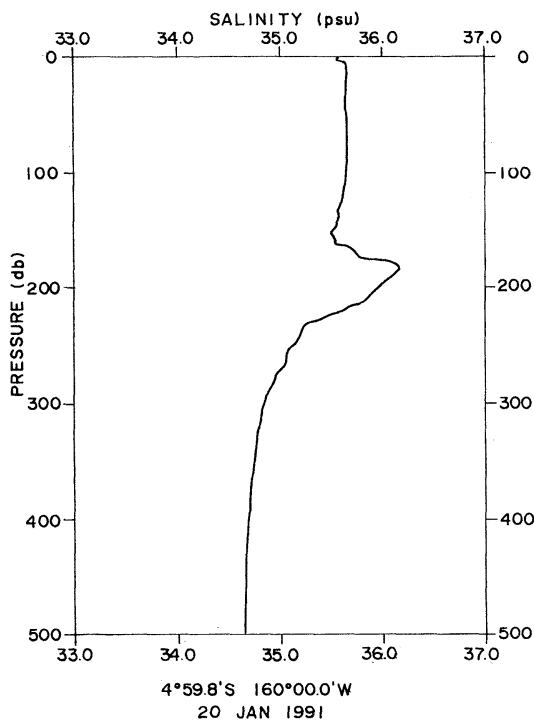## 5. Conclusion

Since publication of the ventilated thermo-

Fig. 7. An example of salinity profile at 5°S 160°W with CTD (Jan. 20, 1991).

cline model by LUYTEN et al. (1983), a number of papers were published both on theoretical and descriptive sides of the subjects. These papers are based on nondissipative dynamics of geophysical fluid. However, the diffusive processes are certainly working in the eastern side of the South Pacific Ocean in the formation of above 36 salinity water, because the thickness of the salinity core increases and the maximum salinity decreases westwards as the subducted water with the high surface salinity is advected.

The JAPACS 1991 cruise data are inadequate to study such processes, particularly because too large longitudinal distances between two meridional sections and also distances from the subduction (subcropping) longitude.
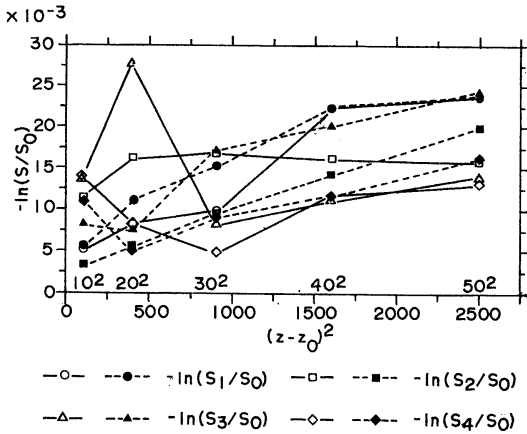
× 10⁻³

Fig. 8. Plots of -ln(S/S_0) versus $(z-z_0)^2$ in m^2.
    S_1 at 160°W, 4°S(S_0=36.10 psu, z_0=180 m),
    S_2 at 160°W, 5°S(S_0=36.15 psu, z_0=180 m),
    S_3 at 180°W, 4°S(S_0=36.08 psu, z_0=180 m),
    S_4 at 180°W, 5°S(S_0=36.18 psu, z_0=190 m).
    Open symbols for positive $z-z_0$ and closed
    symbols for negative $z-z_0$.

contributed substantially to this paper by
redrawing Figs. 2 and 3 and by correcting many
mistakes and inconsistencies of the first draft,
besides typographical erros. If the paper be-
comes readable, we owe it to him.

Appendix
Estimates of K from diffusion equation

Distribution of salinity S advected by current
U in x-direction with diffusivity K is given by
(CRANK, 1956)

$$S = \frac{M}{2\pi\,[K(x-x_s)/U]^{1/2}} \exp\left[-\frac{U(z-z_0)^2}{4K(x-x_s)}\right]$$

(A)

where M is total salt initially concentrated at
$z=z_0$ and at the source point $x=x_s$.

Vertical profiles of salinity from CTD data
during JAPACS 1991 were used to determine the
coefficient of $(z=z_0)^2$ in (A) or

$$\alpha^{-1} = U/4K(x-x_s)$$

(B)

by plotting ln (S/S_0), against $(z-z_0)^2$, where S_0
is salinity at $z=z_0$. The latter can be determined
as a depth of maximum salinity. The longitude
x_s is assumed as the subduction point, though

salinity maximum there is not so sharp as the
plane source indicated by the theoretical curve
of equation(A). Fig. 8 indicates the plot of ln
(S/S_0) versus $(z-z_0)^2$ for S profiles at 160°W.

Two profiles at 160°W are used for α that is
at 5°S and 4°S, whereas z_0 is at 180°W for both
latitudes where Fig. 7 indicates an example of S
at 5°S. The value of K determined from the av-
erage of 5°S and 4°S is 5.5±3.4×10⁻⁵m²/s for U
=10⁻¹m/s. The SD is from different ranges of
curve fitting in $|z-z_0|$. This is the same order
of magnitude as the one determined from the av-
eraged vertical gradient of salinity equation
(5), though number is about 4 times of (5).

The same method applied to 180° profiles of
latitude 5°S (z_0=190m) and 4°S(z_0=180 m)
yields 4.6±3.1×10⁻⁵m/s. These values may be
less reliable than those at 160°W, because the
distance between the supposed source longitude
and the actual stations is too large. However,
the order of magnitudes of K are within a range
of other estimates.

References

ANDO, K., T. ICHIYE and K. MUNEYAMA (1992):
    Watermasses and hydrography in the central
    and western tropical Pacific Ocean. submitted
    to J.Oceanogr.
BUDYKO, M.I.(1974): Climate and Life. Academic
    Press, 508 pp.
COCHRANE, J.D.(1958): The frequency distribution
    of water characteristics in the Pacific Ocean.
    Deep-Sea Res, 5, 111–127.
CRANK, J.(1956): The Mathematics of Diffusion,
    Clarendon Press, Oxford, 347pp.
LEVITUS, S.(1982): Climatological Atlas of World
    Ocean. NOAA Prof. Pap. 13, US Dept. of Com-
    merce, 173 pp.
LUYTEN, J.R., J.PEDLOSKY and H.STOMMEL(1983):
    The ventilation thermocline. J. Phys. Ocean-
    ogr. 13, 1093–1104.
MONTGOMERY, R.B.(1958): Water characteristics of
    the Atlantic Ocean and of the world oceans.
    Deep-Sea Res.5, 134–148.
TSUCHIYA, M.(1968): Upper Water of the Intertrop-
    ical Pacific Ocean. Johns Hopkins Oceanogra-
    phy Studies, Vol.4, 50pp.
WORTHINGTON, L.V.(1982): The water masses of the
    world ocean: Some results of fine-scale cen-
    sus. p.42–69, In: Evolution of Physical Ocean-
    ography, B.A.WARREN and C.WUNSCH (eds),
    MIT Press, 623 pp.

太平洋の 36 psu 以上の高塩分水

市栄　誉, 張　　平

要旨：1991年1〜3月の JAPACS 航海で，南東太平洋の180度以東，南緯30度以北の200 m 深近く及び以浅で36 psu 以上の高塩分水を見いだした．全太平洋でこの塩分範囲の水はこの海域だけである．LEVITUS（1982）の塩分分布図及び土屋（1968）の等比容偏差面（等サーモステリック・アノマリー面）分布図によれば，この水の起源は，赤道と南緯10度との間で西経150度と100度との間の海面の高塩分水が沈降したもののようである．この沈降及び西への移流は西経160度以東，赤道以南の下向きのエクマン・ポンプ流により助長されている．180度線及び西経160度の南緯4度及び5度における塩分の鉛直分布に，水平移流と鉛直拡散の釣り合った式とその解とを適用したところ，鉛直拡散係数の大きさが10^{-5}m^2/s 程度となった．